Structural and optical studies of tin iron chromium nano oxides

M. Kalengay[1*], T.N. Nsio[2]
[1]Department of Mathematics, Sciences and Sports Education, University of Namibia (Rundu)
[2]Department of Integrated Environmental Sciences, Faculty of Agriculture and Natural Resources, University of Namibia, Private Bag 5520 Oshakati, Namibia

ARTICLE INFO

Article history:
Received: 5 February 2019
Received in revised form: 4 March 2019
Accepted: 24 April 2019
Published: 4 November 2019
Edited by KC Chinsembu

Keywords:
Nanoparticles
Hydrothermal method
Structural properties
Optical properties

ABSTRACT

In the present study, we have synthesized $Sn_{0.2}Fe_{0.9}Cr_{0.9}O_3$ nano oxides. Single phase corundum-like structure and nanophase structure of the as-synthesized sample were confirmed by x-ray diffraction (XRD) and by transmission electron microscope (TEM). The results show that the produced powders have grain size of approximately 32 nm. Using the result of the ultraviolet-visible (UV-Vis) spectrometer, we were able to determine the energy band gaps of 3.1 and 5.2 eV , when nanoparticles are diluted in iron standard solution and in deionised water respectively.

1 Introduction

Ferric oxide ($\alpha-Fe_2O_3$), chromic oxide ($\alpha-Cr_2O_3$) and their mixed compounds have applications in many fields. They can be used as catalysts for high temperature water gas shift reaction [1] and reduction of NO_x by NH_3 [2], as refractory materials [3] and sensing materials [4].

Their crystal structure is the same as that of corundum (Al_2O_3). $\alpha-Fe_2O_3$ and $\alpha-Cr_2O_3$ have different semiconducting and sensing properties. Their magnetic and structural properties are influenced by particle size [5, 6], degree of crystallinity [7], pressure [8] and doping [9, 10].

The effect of metal doping by titanium [11, 12], tin [13, 14], manganese [15], aluminium [16, 17], gallium [18] and indium [19] on the electrical, magnetic and other physical properties of $\alpha-Fe_2O_3$ (hematite) has been investigated for some time. The dopant metal ions (tin, titanium) substitute for Fe^{3+} in the corundum-related structure of $\alpha-Fe_2O_3$ with the consequent formation of cationic and anionic vacancies. The difference in ionic radius between the dopant metal ion and that for Fe^{3+} will influence the structural characteristics and phase behaviour of the doped system.

The tin-doped $\alpha-Fe_2O_3$ system has attracted interest because of its sensing properties for gases such as methane and carbon monoxide [20, 21]. The microstructure of tin-doped $\alpha-Fe_2O_3$, prepared by mechanical milling was examined by Jiang et al. [22]. The properties of $\alpha-Cr_2O_3$ can also be drastically changed by varying their size and introducing dopants [23, 24, 25]. Literature suggests that introducing dopants into the sensor material is an effective way to improve sensitivity and selectivity [26]. However, literature on gas sensors based on tin-chromium mixed oxides is rarely available [27, 28].

*Corresponding author: *E-mail address:* MKalengay@unam.na

http://repository.unam.na/handle/11070/790 ISSN: 2026-7673; eISSN: 2026-8653/c 2019 ISTJN.

The substitution of Cr^{3+} by Fe^{3+} to form solid solutions of the type $\alpha-Fe_{2-x}Cr_xO_3$ has been known for some time [29]. Although there have been several studies of the $\alpha-Fe_{2-x}Cr_xO_3$ [21, 29, 30] system, there appears to have been little activity in the doping of these materials by tin. Berry et al. [31] initiated a study of tin-doped oxides of the type $\alpha-Cr_2O_3$ and $\alpha-(FeCr)_2O_3$ and reported on their structural properties.

Therefore, study about effects of these dopants on the structure and optical properties of $(FeCr)_2O_3$ are very important for future applications. In this paper we report the synthesis of $Sn_{0.2}Fe_{0.9}Cr_{0.9}O_3$ using a simple low cost chemical route and study the structure, characterisation and optical absorption properties.

2 Materials and Methods

Single-phase corundum compounds were prepared by mixing an aqueous solution of tin (II) chloride dehydrate with an aqueous solution of chromium (III) chloride hexahydrate and iron (III) chloride hexahydrate. Excess aqueous ammonia was added to the mixtures and the solutions boiled in a stirred pressure reactor for 3 hours. The resulting precipitate was filtered, washed with deionized water until no chloride ions were detected by the silver nitrate standard solution. The precipitate was washed with 95% ethanol and dried under an infrared lamp before calcinations in air at $600°C$ for 12 hours. The products were characterized by X-ray diffraction (XRD) using C_oK_α radiation ($\lambda = 1.7903\,Å$) by a Phillips diffractometer (type: PW1710). A Jeol model JEM-1010 transmission electron microscopy (TEM) was used to obtain the morphology of the samples.

Nano-material (powder) were prepared for spectrophotometric analysis using two different solvents, namely the water de-ionized (H_2O) from UniLab SAARS6725000LL and Iron standard solution, traceable to SRM from NIST $Fe(NO_3)_3$ in HNO_3, (0.5 mol/l). Each substance was accurately weighted using an electronic balance, each sample of 50.0 mg of powder was diluted in 10 ml of solvent. The UV-6300 PC Spectrophotometer (UQE1706002) with a wavelength range of 190-1100 nm at room temperature, was used to record the optical spectrum of the prepared sample. The UV-Vis Analyst-0001 software was used to display the spectrum.

3 Results and discussion

The XRD measurements were scanned in the range $20° \leq 2\theta \leq 80°$ in steps of 0.01/s. The XRD pattern of the as prepared sample of $Sn_{0.2}Fe_{0.9}Cr_{0.9}O_3$ is shown in Figure 1.

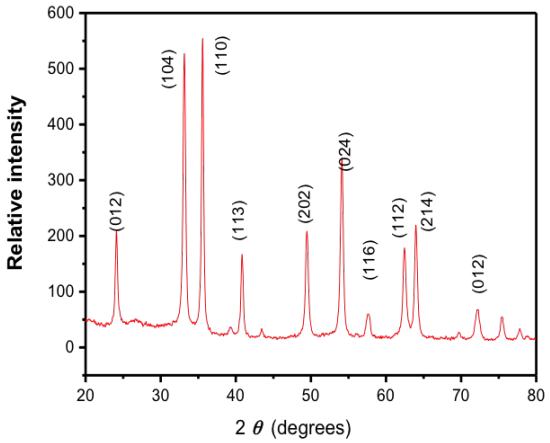

Figure 1: XRD patterns recorded for $Sn_{0.2}Fe_{0.9}Cr_{0.9}O_3$ synthesized in a stirred pressure reactor at $100°C$.

The results are similar to those recorded from tin-doped $\alpha-Fe_2O_3$, $\alpha-Cr_2O_3$ and tin-doped $\alpha-(FeCr)_2O_3$ [20, 23]. The refinement of XRD patterns was then performed by a Rietveld analysis according to an identical model to that was previously used to refine the diffraction data of tin-doped $\alpha-Fe_2O_3$ and $\alpha-Cr_2O_3$ [20]. The structure of $\alpha-Fe_2O_3$ has Fe^{3+} ions distributed in an ordered fashion in $2/3$ of the octahedral sites within a framework of hexagonally close-packed O^{2-} ions. Chains of face sharing octahedral are directed along the c axis, and the Fe^{3+} ions within each chain form pairs as shown in Figure 2.

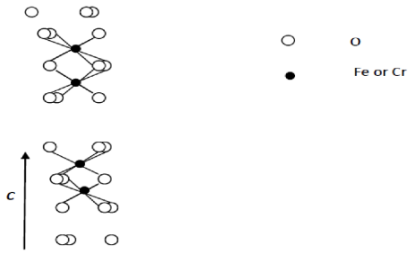

Figure 2: Linking of FeO_6 or CrO_6 octahedra along c in $\alpha-Fe_2O_3$ or $\alpha-Cr_2O_3$.

It was shown [20] that for such structures, the data cannot be fitted to a simple model in which Sn^{4+} substitute for Fe^{3+} with charge balance being achieved by an appropriate number of cations vacancies. The model that we use involves tin ions substituting on two of the octahedral Fe^{3+} sites in corundum related $\alpha-Fe_2O_3$. Elimination of Fe^{3+} cations from the octahedral adjacent to the Sn^{4+} creates two additional octahedral sites that do not involve face sharing and which are therefore amenable to occupation by additional Sn^{4+} ions. The structure is formed by defect clusters comprising a chain of three tin ions which all avoid face-sharing repulsions as shown in Figure 3. The cluster is electrically neutral since 4 Fe^{3+} ions are replaced by 3 Sn^{4+} ions. In the final stage of the refinements, the cation site occupancies were constrained in accordance with the model.

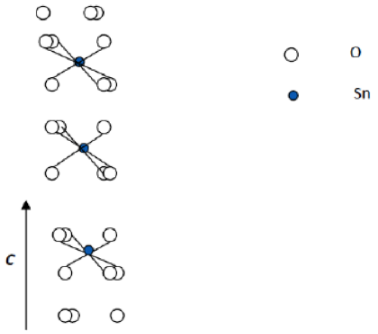

Figure 3: Structural model involving the substitution of 4 Fe^{3+} or 4 Cr^{3+} ions by 3 Sn^{4+} ions.

The measured data and refinement results for $Sn_{0.2}Fe_{0.9}Cr_{0.9}O_3$ are shown in Figure 4, where the black circles indicate the experimental data, red solid line indicates the Rietveld refinement fit by Fullprof analysis software. The green curve at the bottom reveals the difference between the fit and the experimental data.

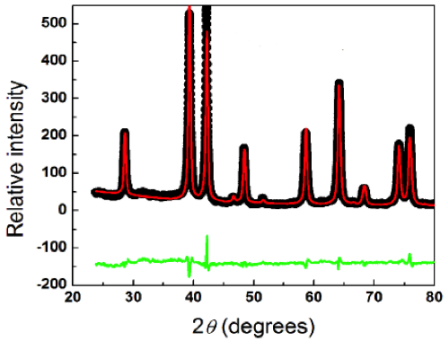

Figure 4: Experimental powder X-ray diffractogram $Sn_{0.2}Fe_{0.9}Cr_{0.9}O_3$ of (black symbols), Rietveld refinement fit (solid red line) and difference curve (green line).

The complete set of final refined parameters are shown in Table 1.

Table 1: Refined Structural Parameters.

Atom	x/a	y/b	x/c	$U_{ISO} \times 100/\text{Å}^2$	Occupancy
CR1	0.00000	0.00000	0.3463(2)	0.500(0)	9.016(2)
Fe	0.00000	0.00000	0.3463(2)	0.500(0)	1.696(2)
Sn1	0.00000	0.00000	0.3463(2)	0.500(0)	0.447(3)
Sn2	0.00000	0.00000	0.00000	0.00000	0.500(0)
O1	0.3217(1)	0.00000	0.2500(0)	0.500(0)	18.000(0)
R_{exp} (%)	14.4	0.00000	R_{exp}	9.5	

The structural parameters show little deviation from those of ideal $\alpha-Fe_2O_3$ and $\alpha-Cr_2O_3$ [31] which suggests that the defect clusters can be incorporated into the corundum structure with very little lattice strain. Direct measurement of the particle size and powder morphology for the as-prepared sample were also performed by transmission electron microscopy (TEM). The TEM image in Figure 5 shows that the sample consists of small nano-sized particles.

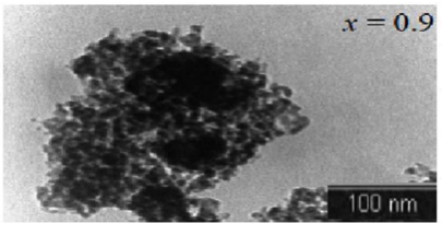

Figure 5: TEM micrograph for the $Sn_{0.2}Fe_{0.9}Cr_{0.9}O_3$ sample.

The calculated D_{XRD} and measured D_{TEM} values appear to be in good agreement. The lattice parameters, the average particle diameters as calculated from XRD data (D_{XRD}) and observed by TEM measurements (D_{TEM}) are shown in Table 2.

Table 2: Particle size (D_{XRD}), (D_{TEM}) and lattice parameters for as-prepared $Sn_{0.2}Fe_{0.9}Cr_{0.9}O_3$ sample.

x	$a = b$ (Å) $\pm 10^{-3}$	c (Å) $\pm 10^{-3}$	V (Å^3) $\pm 10^{-3}$	D_{XRD} (nm) ± 0.4	D_{TEM} (nm) ± 2
0.9	4.981	13.631	291.783	31.5	32

The UV-Vis transmittance and absorbence spectra of the as prepared samples are shown in Figure 6 and Figure 7.

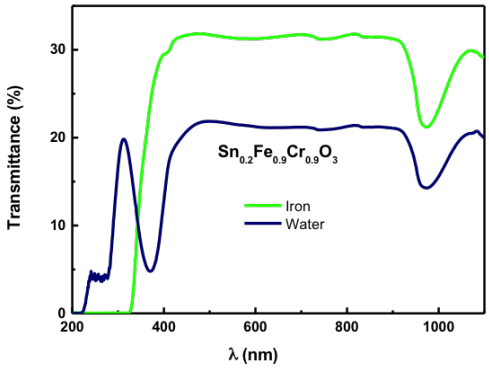

Figure 6: UV-vis transmittance spectrum of $Sn_{0.2}Fe_{0.9}Cr_{0.9}O_3$ nanoparticles.

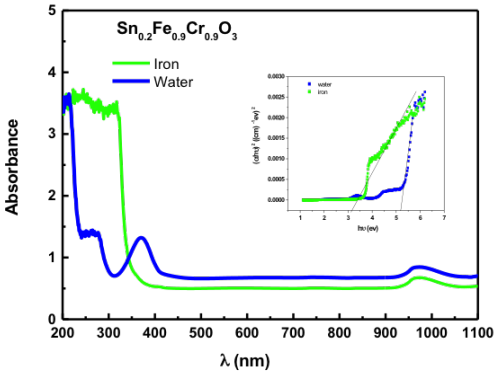

Figure 7: UV-vis absorbance spectrum of $Sn_{0.2}Fe_{0.9}Cr_{0.9}O_3$ nanoparticles. Inset shows the determination of optical bandgap energies for the respective nanoparticles.

The transmittance spectrum of the prepared $Sn_{0.2}Fe_{0.9}Cr_{0.9}O_3$ shows that, in both the UV (400 nm) and visible (400-800 nm) regions the sample is having high transparency and its transmittance is lower for the sample diluted in water. The absorbance spectrum of the sample shows that the absorption edge shifted towards longer wavelengths (red shifted) from 250 to 350 nm from the sample diluted in water to the one with the Fe

concentration. The optical band gap energy (E_g) of the as-synthesized nanoparticles is obtained from the UV-Vis spectra by using a well-known Tauc's relation [32]:

$$(\alpha hv) = A(hv - E_g)^n, \tag{1}$$

where α is the absorption coefficient, A is a constant, E_g is the band gap energy of the material and exponent $n = \frac{1}{2}$ for direct transition. The value of the absorption coefficient can be determined by the following equation [33]:

$$\alpha = 2.303\left(\frac{\text{absorbance}}{t}\right), \tag{2}$$

where 't' is the thickness of the sample. The curves are plotted between $(\alpha hv)^2$ versus (hv) and extrapolating of the linear portions of the curves to the hv axis gives $E_g = 3.1$ eV for the sample diluted in iron solvent which is in agreement with the reported values by Huagiang, et al., [34] and 5.2 eV for the sample diluted in deionised water as shown in the inset of Figure 7.

4 Conclusion

$Sn_{0.2}Fe_{0.9}Cr_{0.9}O_3$ fine powders have been successfully synthesized by hydrothermal process at low temperature ($100°$C) and annealed at $600°$C. The XRD patterns indicate that the sample has single phase. The crystallite size calculated from XRD data shows good agreement with the particle size obtained by TEM. The absorbance spectrum of the prepared sample shows that the absorption edge shifted towards longer wavelengths (red shifted) from 250 to 350 nm when the sample is diluted in iron standard solution with an energy gap of 3.1 eV.

Acknowledgements

We acknowledge the condensed matter group University of KwaZulu-Natal (UKZN) for measurements and the support from the University of Namibia (UNAM).

References

[1] D. Christopher, K. Amit Agrawal, C. Erick Walter and D. Mark Vaudin, "Effect pf Tin doping on hematite photoanodes for water splitting," *Journal of Physical Chemistry C*, vol. 116, no. 29, pp. 15290–15296, 2012.

[2] R. J. Willey, H. Lai and J. B. Peri, "Investigation of iron oxide-chromia-alumina aerogels for the selective catalytic reduction of nitric oxide by amonia," *Journal of Catalysis*, vol. 130, no. 2, pp. 319–331, 1991.

[3] A. Muan and S. Omiya, "Phase relations in the system iron oxide Cr_2O_3 in air," *Journal of the American Ceramic Society*, vol. 43, no. 4, pp. 204–209, 1960.

[4] Y. Shimizu, S. Kusano, H. Kuwayama, K. Tanaka and M. Egashira, "Oxygen sensing properties of spinel-type oxides for stoichiometric air/fuel combustion control," *Journal of American Ceramic Society*, vol. 73, no. 4, pp. 818–824, 1990.

[5] A. S. Teja and K. Pei-Yoong, "Synthesis, properties and applications of magnetic iron oxide nanoparticles," *Progress in Crystal Growth and Characterization of Materials*, vol. 55, no. 1–2, pp. 22–45, 2009.

[6] S. J. Stewart , R. A. Borzi, E. D. Cabanillas, G. Punte and R. C. Mercader, "Effect of milling-induced disorder on the lattice parameters and magnetic properties of hematite," *Journal of Magnetism and Magnetic Materials*, vol. 260, no. 3, pp. 447–454, 2003.

[7] D. G. Rancourt, J. E. Dutrizac, G. Lamarche, R. Provencher and M. Z. Dang, "Interplay of surface conditions, particles size, stoichiometry, cell parameters and magnetism in sythetic hematite-like materials," *Hyperfine Interact*, vol. 117, no. 271, 1998.

[8] C. L. Bruzzone and R. Ingalls, "Mössbauer-effect study of the Morin transition and atomic positions in hematite under pressure," *Phys. Rev. B*, vol. 28, pp. 2430–2440, 1983.

[9] C. A. Barrero, J. Arpe, E. E. Sileo, L. C. Sanchez, R. Zysler and C. Saragovi, "Ni-and Zn-doped hematite obtained by combustion of mixed metal oxinates," *Physica B: Condensed Matter*, vol. 354, no. 1, pp. 27–34, 2004.

[10] E. E. Sileo, D. Perez, A. Cesar, L. Larralde, S. Mariela and C. Saragovi, "Influence of the genesis on the structural and hyperfine properties of Cr-substituted hematites," *Chemical Geology*, vol. 238, no. 1–2, pp. 84–93, 2007.

[11] J. Morin, "Electrical properties of Fe_2O_3 and $\alpha-Fe_2O_3$ containing titanium," *Phys. Rev. B*, vol. 83, pp. 1005–1010, 1951.

[12] M. Watanabe, K. Kaneko , N. Uekawa and F. Mizukami, "Mixed-valence formation in highly oriented Ti-doped iron oxide film.," *J. Chem. Soc,* vol. 91, p. 2161, 1995.

[13] P. B. Fabritchnyi, E. V. Lamykin, A. M. Babechkin and A. N. Nesmeianov, "Study of Morin transition by Mössbauer effect in hematite contening Tin impurity," *Solid State Communications*, vol. 11, no. 2, pp. 343–348, 1972.

[14] K. Melzer, H. Mehner, F. Schneider and G. Deke, "Study of local spin structure in singly substituted YIG ferrites," *Phys. Stat. Sol. (a)*, vol. 39, no. 2, pp. 643–650, 1977.

[15] S. Popovic, M. Metkos-Hukovic, S. Music and G. Gvozdic, "X-ray absorption study on the local structures of fine particles of $\alpha-Fe_2O_3$ gas sensors," *J. Mater. Chem*, vol. 2, p. 703, 1992.

[16] E. D. Grave, D. Chambaere and L. H. Bowen, "Nature of the Morin transition in Al-substituted hematite," *Journal of Magnetism and Magnetic Materials*, vol. 30, no. 3, pp. 349–354, 1983.

[17] S. A. Fysh and P. E. Clark, "A Mössbauer study," *Physics and Chemistry of Minerals*, vol. 8, no. 6, pp. 257–267, 1982.

[18] S. Music, S. Popovic and M. Ristic, "X-ray diffraction and Mössbauer spectra of the system Ga_2O_3," *Journal of Materials Science*, vol. 24, pp. 2722–2726, 1989.

[19] M. Ristic, S. Popovic, M. Tonkovic and S. Music, "Chemical and structural properties of the system Fe_2O_3 - In_2O_3," *Journal of Materials Science*, vol. 249, no. 15, pp. 4225–4233, 1991.

[20] I. Ayub, C. Johnson, D. A. Johnson, E. A. Moore, X. Ren and H. M. Widatallah, "Tin-, titanium-, and magnesium-doped $\alpha-Cr_2O_3$: characterisation and rationalisation of the structures," *Solid State Communications*, vol. 123, no. 3–4, pp. 141–145, 2002.

[21] W. Zhu, M. S. Tse, Y. Liu and S. Y. Shen, "Study of new alcohol gas sensors made from ultrafine SnO_2 - Fe_2O_3," *Journal of Materials Sciences Letters,* vol. 249, no. 14, pp. 1185–1187, 1995.

[22] J. Z. Jiang, R. Lin , K. Nielsen, S. Morup, D. G. Rickerby and R. Clasen, "Interstitial positions of tin ions in $\alpha-FeSn_2O_3$ solid solutions prepared by mechanical alloying," *Phys. Rev. B*, vol. 55, no. 22, pp. 14830–14835, 1997.

[23] F. J. Berry, C. Greaves, O. Helgason, J. McManus, H. M. Palmer and T. R. Williams, "Structural and magnetic properties of Sn, Ti, and Mg-substituted $\alpha-Fe_2O_3$: A study by neutron diffraction and Mössbauer spectroscopy," *Journal of Solid State Chemistry*, vol. 151, no. 2, pp. 157–162, 2000.

[24] F. M. Filho, A. Z. Simes, A. Ries, L. Perazolli, E. Longo and J. A. Varela, "Nonlinear electrical behaviour of the Cr_2O_3, ZnO, CoO and Ta_2O_5-doped SnO_2 varistors," *Ceramics International*, vol. 32, no. 3, pp. 2833–289, 2006.

[25] A. Stashans and S. Jacome, "Local structure, magnetic and electronic properties of N-doped $\alpha-Cr_2O_3$ from the first-principles," *Computational Materials Science*, vol. 81, pp. 353–357, 2014.

[26] K. Zakrzewska, "Mixed oxides as gas sensors," *Thin Solid Film: Proceedings of the 2nd International Seminar on Semiconductor Gas Sensors*, vol. 391, no. 2, pp. 229–238, 2001.

[27] P. T. Moseley and D. E. Williams, "A selective ammonia sensor," *Sensors and Actuators B: Chemical*, vol. 1, no. 1–6, pp. 113–115, 1990.

[28] W. Zeng, T. Liu, D. Liu and E. Han, "Hydrogen sensing and mechanism of doped SnO_2 nanocomposite," *Sensors and Actuators B: Chemical*, vol. 160, no. 1, pp. 455–562, 2011.

[29] J. K. Srivastava, G. K. Shenoy and R. P. Shama, "Magnetic structure of Cr_2O_3 - Fe_2O_3 system," *Solid State Communications*, vol. 6, no. 2, p. 73–76, 1968.

[30] A. K. Bhattacharya, C. K. Majumdar, D. Chintalapudi and A. Hartridge, "A Mossbauer study of Fe_2O_3 - Cr_2O_3 nanocrystals dispersed in a silica matrix," *Journal of Magnetism and Magnetic Materials*, p. 183, 1998.

[31] F. J. Berry, O. Helgason, T. Moyo and X. Ren, "Tin doping of $\alpha-Cr_2O_3$ and $\alpha-(FeCr)_2O_3$," *Journal of Materials Sciences Letters*, vol. 59, no. 26, pp. 3241–3245, 2005.

[32] J. Tauc, Amorphous and liquid semiconductors, New York: Plenum, 1974.

[33] J. W. Robinson, Atomic Spectroscopy, 2nd Edition ed., New York: Taylor & Francis, 1996.

[34] C. Huaqiang, Q. Xianqing, L. Yu, Z. Meijuan and Z. Qiming, "Sol-gel synthesis and photoluminescence of p-type semiconductor Cr_2O_3 nanowires," *Applied Physics Letters*, vol. 88, no. 24, p. 241112 (3), 2006.